

Study on Electrochemical Impedance Response of Sulfate Saline Soil

Peng Shuquan*, Wang Fan and Fan Ling

School of Resources and Safety Engineering, Central South University, Changsha, 410083

*E-mail: pqr97linger@csu.edu.cn

Received: 4 April 2019 / Accepted: 25 June 2019 / Published: 31 July 2019

Since salt expansion of sulfate saline soil has great adverse effects on the engineering, it is significant to conduct the non-destructive test of salinity and water content of sulfate saline soil in the treatment process. To accurately detect the variation, electrochemical impedance characteristics of sodium sulfate content and water content in sulfate saline soil were studied by Electrochemical Impedance Spectroscopy (EIS), and the response strain of electrical impedance in sulfate saline soil was obtained under different salinity and water content. Through the data fitting of Zview software, the corresponding Bode and Nyquist diagrams were obtained, and the equivalent circuit model (ECM) was correspondingly analyzed to obtain the electrical impedance variation law of sulfate saline soil under different conditions of salinity and water content. The experimental results show that the electrical impedance modulus ($|Z|$) decreases with the increase of salinity and water content of sulfate saline soil. By evaluating and calibrating the $|Z|$ of sulfate saline soil under different water content and salinity conditions, the negative exponential relationship between the partial total resistance of the soil pore solution (R_1) and the connected micro-pore resistance (R_2) of the equivalent circuit element and the water content and salinity were obtained. Positive exponential correlation with a contact interface capacitance (CPE); and the prediction equations of water content and salinity of sulfate saline soil were deduced by using R_1 and R_2 . This study further enriches the application of EIS technology in geotechnical engineering.

Keywords: EIS; sulfate saline soil; salinity; water content; ECM.

1. INTRODUCTION

The determination of salinity and water content in saline soil is an important research topic. One of the most important applications of salinity and water content measurement is to estimate the concentration of sodium sulfate in sulfate saline soil so as to accurately evaluate its salt expansion behavior [1-2]. Previous studies have shown that under the influence of salinity and water content [3-

6], salt expansion causes severe damage to buildings, geotechnical engineering, and the environment [7-8]. Accurate estimation of its salinity and water content is of considerable significance to the protection of buildings and the environment.

Electrochemical impedance spectroscopy (EIS) which is a non-destructive, efficient and real-time measurement method [9-13] can be used for soil electrical impedance measurement [14-15]. Electrical impedance is a part of the main characteristics of soil, which is affected by soil particles, salinity, water content, soil type, and other factors. The equivalent circuit model (ECM) is an essential tool for electrical impedance measurement [16].

The ECM [17, 18] can be used to fit and determine the relationship between the measured electrical impedance and the circuit element parameters (R_1 , R_2 , and C) in the ECM. Previous studies showed that EIS was used to measure the electrical impedance of soil with different water contents, and the results were analyzed accurately according to the corresponding ECM [12]. In addition, EIS was used to test the soil particle size [19], salt ion concentration [20], soil water characteristic curve [21]. These results serve in engineering practice and soil research well. According to the above research, EIS is a feasible and effective method to measure soil characteristic parameters. It is also likely to be effective to detect sulfate saline soil and can be used to detect sulfate saline soil particles and pores [19]. However, as far as we know, there is no other document describing how to measure the electrical impedance of sulfate saline soil with different salinity and water content by EIS. Compared with the traditional pretreatment method, this method does not require any pretreatment, which brings more convenience to the measurement work.

In this paper, sulfate saline soil samples are prepared manually. EIS tests are used to study the electrical impedance response of the system in the frequency range of 0.1-10⁵ Hz, and the corresponding ECM is analyzed. The magnitude of impedance ($|Z|$) of the system which changes rule with the water content and salinity of sulfate saline soil is described. An electrochemical impedance spectroscopy (EIS) method to measure water content and salinity of sulfate saline soil is proposed, and the ECM elements (R_1 , R_2 , and C) based on soil and the calculation equations of salinity and water content are further derived. This study is of great significance to the research and treatment of soil salt expansion and the development of environmental impact assessment technology.

2. EXPERIMENTAL PROCEDURE

2.1 Sample preparation and test scheme

Standard sand and pure anhydrous sodium sulfate were used to prepare the sulfate saline soil. Standard sand is produced by Xiamen ISO Standard Sand Co. Ltd, China. Fig.1 shows the specific grain gradation curve. The particle size ranges from 0.08 mm to 2.00mm, the inhomogeneity coefficient is 6.25 and the curvature coefficient is 1.56. According to ASTM standards [22], the sand was a well-graded soil. Tab.1 shows the basic chemical composition. Anhydrous sodium sulfate is 99% analytical purity (CAS: 7757-82-6) produced by China National Pharmaceutical Group Corporation.

Table 1. Basic chemical composition of standard ISO sand

Sample	SiO ₂	Fe ₂ O ₃	Al ₂ O ₃	CaO	MgO	Others
Content/%	98.6	0.1	0.8	0.1	0.1	0.3

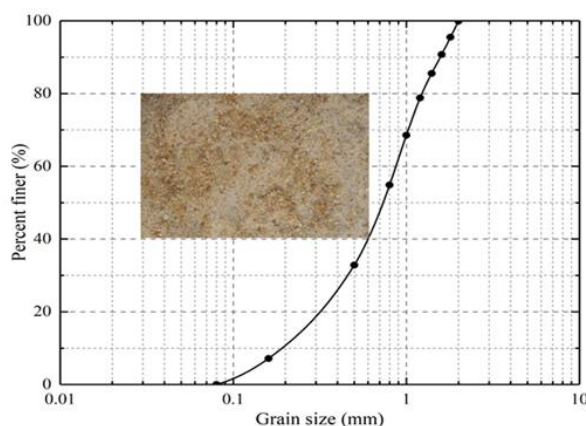


Figure 1. Grain size distribution for standard test ISO sand

Table 2. Basic physical properties of sulfate saline soil samples (salinity: 0~6%; water content: 0~30%)

Sample/No	Salt Content(Na ₂ SO ₄)/%							
	0	1	2	3	4	5	6	
Water Content /%	0	A-1	B-1	C-1	D-1	E-1	F-1	G-1
	5	A-2	B-2	C-2	D-2	E-2	F-2	G-2
	10	A-3	B-3	C-3	D-3	E-3	F-3	G-3
	15	A-4	B-4	C-4	D-4	E-4	F-4	G-4
	20	A-5	B-5	C-5	D-5	E-5	F-5	G-5
	25	A-6	B-6	C-6	D-6	E-6	F-6	G-6
	30	A-7	B-7	C-7	D-7	E-7	F-7	G-7

The standard sand and anhydrous sodium sulfate were dried in the drying oven at 105°C for 48 hours, cooled down to room temperature, and then preserved in a polymer bag immediately for the drying. Then, the standard sand and anhydrous sodium sulfate were weighed by electronic scales, packed in containers and stirred for 30 minutes at a rate of 150 r/s by a small mixer, so as to distribute the salt evenly. Then sulfate saline soil samples were prepared. After evenly adding deionized water, 7 samples of sulfate saline soil with different parameters of water content (an interval of 5%, the range of 0-30%) and 7 samples of sulfate saline soil with different parameters of sodium sulfate content (an interval of 1% and the range of 0-6%) were prepared. Tab.2 shows the detailed samples of sulfate saline soil. After sufficient agitation, the soil samples were placed in a plastic mold with an inner diameter of 50 mm, a thickness of 5mm and a height of 100 mm. A self-made tramper of 300 ± 0.5 g was used to drop freely from a height of 100 mm, and then the sulfate saline soil sample was compacted with a density of 2.20 g/cm³. Then samples were sealed with the sealing film and placed in

the temperature and humidity chamber for 24 hours. After the steady forming and the uniform salt distribution, the measurement was conducted.

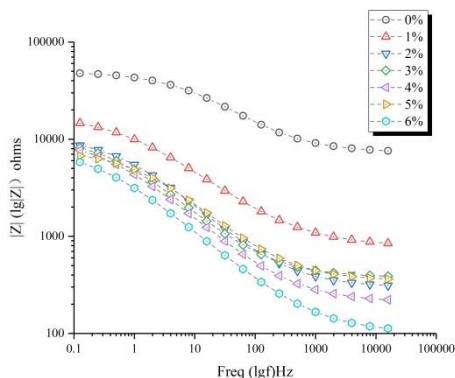
2.2. Test procedures

The electrochemical workstation model (PARSTAT 3000A-DX) is used in the test. Its electrodes are used to connect the sample to the instrument. To ensure full contact and good conductivity, copper sheets were used to connect the samples and instruments. Before testing the impedance parameters, the copper sheets should be cleaned and polished to minimize the contact resistance. The surface of the test sheets should be treated smoothly to ensure close contact. Threaded rods were mainly used to ensure sufficient connection between samples and copper sheets. The protruding end of copper sheets was connected to the test electrode. The reference electrode (RE) and counter electrode (CE) were connected with the upper copper sheet, and working electrode (WE) and the sense electrode (SE) were connected with the lower copper sheet[17, 23]. Square plexiglass was placed between the two copper sheets and the fixed bracket to prevent the diffusion of tested alternating current (AC).

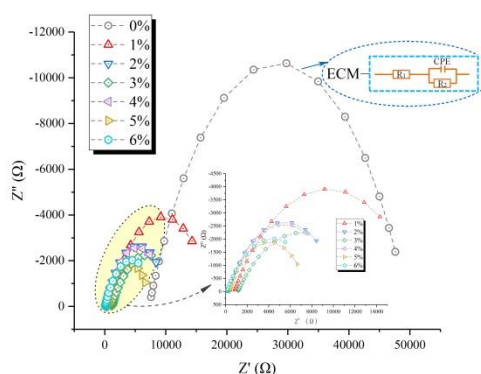
The frequency range for the testing sample was adjusted to 10^{-1} - 10^5 Hz and the voltage signal was 10mV in the measurement. After setting the start-up program of the relevant test parameters, the real part, imaginary part, modulus, and phase angle of the sample impedance were measured by the automatic frequency scanning to complete AC impedance spectrum measurement. Bode and Nyquist diagrams were obtained and then fitted with Zview software [9,19]. In addition, by analyzing the ECM, a close mathematical relationship between circuit element parameters and salinity and water content of sulfate saline soil are established. The inversion calculation of salinity and water content in sulfate saline soil is realized by using mathematical equation.

3. RESULTS AND DISCUSSION

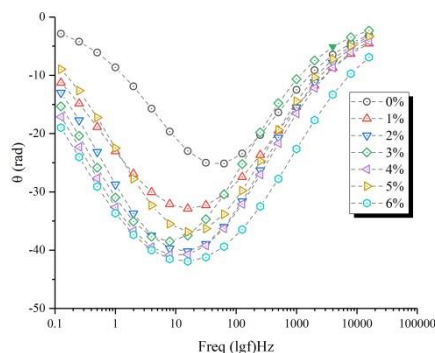
3.1 Effect of salinity



(a) Impedance mode value diagram (Bode plots)



(b) Nyquist plots



(c) Phase angle graph

Figure 2. EIS diagram ($f=0.1\sim 10^5\text{Hz}$) of sulfate saline soil with different salinity (0~6%) under 10% water content. ((a).Impedance mode value diagram (Bode plots), (b).Nyquist plots, (c). Phase angle graph)

According to Tab.2, test results of sulfate saline soil samples with 10% water content and salinity from 0% to 6% are obtained. Fig. 2(a) shows that, with the increase of frequency, the $|Z|$ of sulfate saline soil decreases, under salinity from 0% to 6%, and similar $|Z|$ reduction curves can be obtained. Since the capacitance has the characteristics of passing high-frequency blocking low-frequency in the ECM, when the frequency is high, the $|Z|$ is reduced. Fig. 2(a) shows that the electrical $|Z|$ of sulfate saline soil decreases with the increase of salinity.

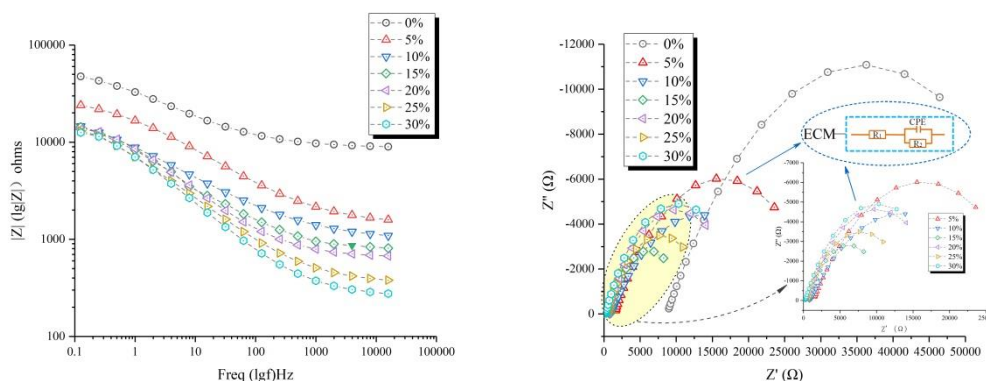
Fig. 2(b) shows the measured parameters of the real part (Z') and the imaginary part (Z'') of the impedance through the test. The results demonstrate that the absolute value of the imaginary part of the impedance firstly increases and then decreases with the increase of frequency, and both of them are semi-circular. The maximum absolute value of the imaginary part of the impedance decreases with the increase of salinity. As salinity decreases, the area enclosed by Z' and Z'' gradually decreases. Since the increase of salinity leads to the growth of ion concentration in the soil sample, the resistance is reduced.

Fig. 2(c) shows that the absolute value of phase angle increases with the increase of salinity and frequency in the low-frequency band ($f < 10\text{ Hz}$), while it decreases in the high-frequency band ($f > 1000\text{ Hz}$). This is because, with the increase of salinity, the ion concentration in the soil sample increases, which shortens the power supply time of capacitance between the test copper sheet and soil sample. Thus, the phase angle is changed correspondingly [14, 16, 23].

3.2 Effect of water content

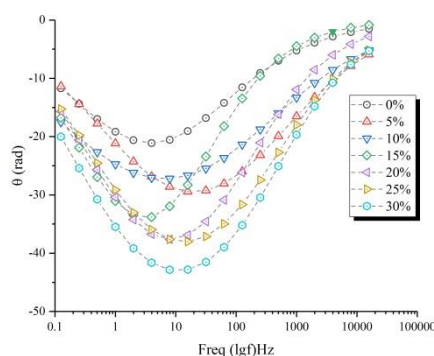
According to Tab.2, test results of the sulfate saline soil sample with 3% salinity are obtained under the water content in the range of 0% to 30%. Fig. 3(a) shows that, with the frequency increases, the $|Z|$ of the sulfate saline soil with different water content decreases, and a similar $|Z|$ reduction curve can be measured. In addition, it shows that the $|Z|$ of sulfate saline soil decreases with the increase of water content, which is consistent with the variation law of water content studied by Lesmes [20].

Since the rise of water content leads to the increase of solution volume in the soil sample, the void of soil sample decreases relatively, and soil sample is closer to the electrochemical solution system. Thus, the measured $|Z|$ decreases.



(a) Impedance mode value diagram (Bode plots)

(b) Nyquist plots



(c) Phase angle graph

Figure 3. EIS diagram ($f=0.1\sim 10^5$ Hz) of sulfate saline soil with different water content (0~30%) under 3% salinity. ((a).Impedance mode value diagram (Bode plots), (b).Nyquist plots, (c). Phase angle graph).

Fig. 3(b) shows the measured parameters of the real part and the imaginary part of the impedance by the experiment. The results demonstrate that the absolute value of the imaginary part firstly increases and then decreases, both of them are semi-circle shape. With the increase of water content, the radius of the circle gradually decreases.

The absolute value of the phase angle decreases with the increase of the water content, as can be seen from Fig. 3(c). The absolute value of phase angle increases with the increase of frequency in the low-frequency band and decreases with the increase of frequency in the high-frequency band, which is consistent with the changing trend of salt content. As water content increases, the volume of solution in soil sample also increases, while the ion concentration in soil sample decreases, so that the phase angle changes little. With the further increase of water content, the void volume of soil sample decreases. Thus the powers supply time of measuring the capacitance decreases and the phase angle decreases [16, 24].

3.3 The establishment of parameter elements of ECM in sulfate saline soil

The composition of the soil determines its conductive step, and the corresponding ECM can be established according to the conductive steps. Previous studies have demonstrated that there are three conductive steps in the soil structure (Fig.4): discontinuous conductive steps between soil particles and pores, conductive steps between continuous soil particles, and conductive steps between continuous pore [12, 16, 23, 24]. The porosity of soil is expressed by pure resistance. The granular part of the soil is represented by a parallel combination of capacitance and resistance. Particle-core part of the soil is represented by the parallel connection of capacitance and resistance and the series connection of resistance (Fig.4). In most cases, the resistivity of soil particles in soil microstructure is very high, and the resistance in the parallel combination can be ignored (Fig.4) [3, 16, 23]. Due to the continuity of three conductive steps, the components of the soil circuit are connected in series. The ECM can also be simplified to a conventional ECM and has the same EIS curves [23, 24]. Due to the fact that the capacitance of soil particles is difficult to be accurately obtained in the test process and the value is very small, it can be further simplified $C_{CSS} \approx 0$ (Fig.4) [24]. The "dispersion effect" is a common phenomenon that the test curve deviates from the semicircle track during the EIS experiment, which further complicates the capacitance expression. Therefore, the constant phase angle element (CPE) is used to replace the capacitor, and the simplified equivalent circuit model, which makes it closer to the actual impedance spectrum [25]. The simplified ECM (Fig.4) obtained from the three-phase composition of saline soil is in good agreement with the ECM obtained by fitting the experimental results (Fig.2; Fig.3), further verifying the accuracy and importance of each parameter element.

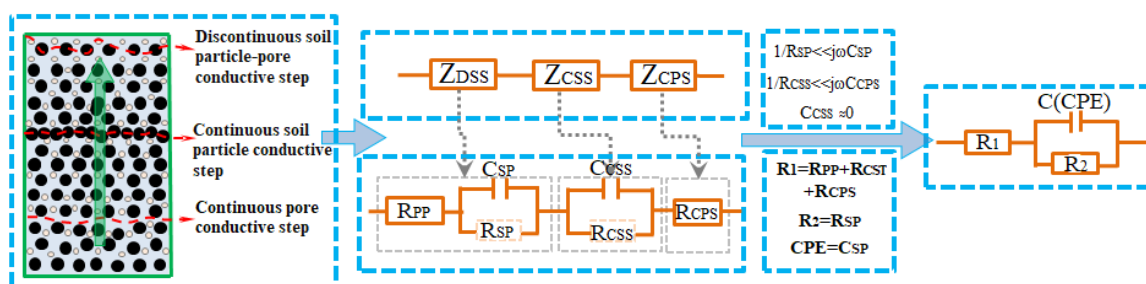


Figure 4. Equivalent circuit model: Where it is the process of converting the three-phase composition of the soil into an equivalent circuit. (The salinity changes range of sulfate saline soil, is 0~6%. The water content changes range of sulfate saline soil, is 0~30%). Z_{DSPP} - Impedance of discontinuous soil particle-pore conductive step (DSPP). Z_{CSS} - Impedance of continuous soil particle conductive step (CSS). Z_{CPS} - Impedance of continuous pore conductive step (CPS). j is the rotation factor of 90 degrees in impedance. ω - Angular frequency ($\omega = 2\pi f$). R_{PP} - Resistance of continuous pore step portion of DSPP. R_{SP} - Resistance of soil particle portion of DSPP. R_{CPS} - Resistance of continuous pore conductive steps (CPS). R_{CSS} - Resistance of continuous soil particle conductive steps (CSS) C_{CSS} - Capacitance of continuous soil particles step in soil. C_{SP} - Capacitance of soil particle portion of DSPP.

When the sulfate saline soil samples are measured by EIS, corresponding equivalent circuits are formed among the conductive steps of the soil. When the salinity and water content of sulfate

saline soil change, the parameter values of circuit elements (an overall resistance of a soil pore solution part (R_1), a connected micro-pore resistance (R_2) and a contacted interface capacitance (C)) of the equivalent circuit will also change (Fig.4). Therefore, by determining the electrical impedance of the equivalent circuit, the salt content and water content of sulfate saline soil can be obtained through inversion analysis.

3.4 Establishment of salinity and water content prediction equation for sulfate saline soil by EIS technology

Based on the measured results and the ECM (Fig.4), the corresponding mathematical equations (Eq.1~3) between R_1 , R_2 and C were established which could accurately and effectively evaluate soil salinity and water content [12, 16, 23]. Based on the ECM, the influence law of salinity and water content of sulfate saline soil on the electrical impedance of the system is analyzed, and the electrochemical impedance measurement equation of salinity and water content of sulfate saline soil is obtained by least square fitting.

3.4.1 Relationship between Water Content and R_1 , R_2 , and C in ECM

Table 3. The relation between water content (W: 0~30%), salinity (W_s : 0~6%) and R_1 in the ECM of sulfate saline soil

W%($R_1 \sim \Omega$)	$W_s\%$						
	0	1	2	3	4	5	6
0	5289	4957	4613	4399	4250	4160	4077
5	3999	3704	3513	3358	3255	3166	3099
10	3012	2893	2765	2679	2549	2425	2388
15	2321	2171	2100	1954	1801	1699	1603
20	1529	1439	1355	1285	1232	1167	1127
25	1099	1042	930	877	822	744	688
30	605	502	410	347	282.5	256.5	237.5

Table 4. The relation between water content (W: 0~30%), salinity (W_s : 0~6%) and R_2 in the ECM of sulfate saline soil

W%($R_2 \sim k\Omega$)	$W_s\%$						
	0	1	2	3	4	5	6
0	1675	1491	1332	1200	1113	1065	988
5	831.4	742	667	580	511	488	451
10	388	300	220	170	140	126	119.8
15	116.4	109.4	104.5	100.1	96.6	93.3	89.1
20	86	80.2	76.1	72	68	65.3	63
25	60.1	55	49	45.52	43.5	41	39
30	35	31	26.5	22.5	20.76	19.55	18.65

Table 5. The relation between water content (W: 0~30%), salinity (W_s: 0~6%) and C in the ECM of sulfate saline soil

W%(C~μF)	W _s %						
	0	1	2	3	4	5	6
0	0.24	0.28	0.33	0.38	0.43	0.5	0.61
5	0.65	0.7	0.77	0.84	0.98	1.1	1.23
10	1.28	1.36	1.46	1.58	1.8	2.13	2.6
15	2.62	2.68	2.87	3.08	3.6	4.2	5.3
20	5.33	5.99	6.3	6.9	7.5	8.92	10.6
25	10.69	10.78	11.12	12.9	14.5	17.2	21.2
30	21.8	25.22	31.44	36.2	44.7	51.4	58.2

Tab.3 and Tab.4 show that R_1 and R_2 of sulfate saline soil samples with the same thickness ($L=10\text{cm}$) decrease significantly with the increase of water content, and have an exponential relationship with water content (W% represents water content). In order to explain the above phenomenon, referring to the specific model, R_1 is mainly attributed to the resistance of the pore solution, and R_2 is attributed to the resistance of the interface between the hydration product and the pore solution [26-28]. Increasing the water content is equivalent to increasing the solution content in the soil and accelerating the movement of solution ions. Externally, the values of R_1 and R_2 decrease.

The increase of water content will significantly reduce the resistance R_1 of the pore solution, while the reduction degree of resistance R_2 is much smaller, which can be assessed by the figures of Tabs.3~5. However, Tab.5 shows that with the increase of water content, the interfacial capacitance C increases significantly as an exponential relationship, and accelerates the electrochemical charge-discharge reaction of soil [20].

3.4.2 Relationship between Salinity and R_1 , R_2 and C in ECM

Tab.3 and Tab.4 show that R_1 and R_2 decrease with the increase of salinity and change in the exponential relationship with salinity (W_s% represents salinity) for sulfate saline soil samples under the same initial conditions. This shows the same change trend as water content, but the curve change tendency shows that the effect of water content on soil sample resistance is more prominent. Increasing salinity is tantamount to increasing the ion content of the solution in the soil and enhancing the ion migration movement. The results show that the values of R_1 and R_2 are significantly reduced. The increase of salinity will reduce the resistance R_1 of pore solution, while the reduction degree of interfacial resistance R_2 is not much different, which can be judged by the figures of Tabs.3~5.

Tab.5 shows that the interfacial capacitance increases exponentially with the salinity. Compared with the increase and change of water content, the effect of water content on capacitance is more significant, while the effect of salinity on capacitance is much smaller. As water content increases results in the total amount of solution increases, while the increase in salinity is the increase

in salt concentration. The change of solution has a significant impact on ion migration and chemical charge-discharge reaction [12, 20, 23].

Both water content and salinity have significant effects on the circuit components R_1 , R_2 , and C in the equivalent circuit model [12, 16]. However, the increase of water content is often accompanied by the increase of solution volume, which has a significant effect on the solution resistance. Under the action of alternating current, the migration movement of ions is enhanced, and the volume of pores in the sulfate saline soil is reduced. It promotes the ions to migrate from the solution to the interface and further affects the interface resistance and capacitance. The increase of salinity significantly increases the ion concentration, but in the ion migration and interface migration, the priority of water content is much higher than that of salinity, which is well proved in the above test results [23, 24, 27-29].

3.4.3 Relationship between salinity, water content and electrical impedance in ECM and solution of prediction equation

The above results demonstrate that changes in salinity and water content will lead to corresponding exponential changes in R_1 and R_2 in the ECM [6, 12, 30]. The experimental results show that when the change rule between R_1 and R_2 and the salinity and water content is reflected in a quantitative exponential relationship, the test results of R_1 and R_2 of the soil can reflect its salinity and water content.

According to the previous data analysis of the relevant test results in the previous section, the prediction equation of electrical impedance under the interaction of 7 water content change factors and 7 salinity change factors is obtained by combining the results of the uniform test (see Tab.2). When the unified test results of equation 1 and equation 2 are fitted, the values of water content and salinity are solved at the same time. Tabs.3~5 shows the change rule of the electrical impedance value of sulfate saline soil with the change of water content and salinity, and equation 3 is obtained through nonlinear data-fitting. The digital relationship between water content, salinity, and electrical impedance value is established, and the prediction equation between water content, salinity and electrical impedance value is fitted.

Equation 3 can well fit and explain the non-linear change rule of the electrical impedance value of sulfate saline soil under the environment of different water content and salinity. Through testing soil R_1 and R_2 , the inversion calculation of water content and salinity of the tested soil sample can be realized.

$$R_1 = -1697.36 + 6773.11 \cdot e^{\left(\frac{W_S\%}{34.24} - \frac{W\%}{27.83}\right)}; R^2 = 0.9976 \quad (1)$$

$$R_2 = 8.55 + 1662.93 \cdot e^{\left(-\frac{W_S\%}{10.2} - \frac{W\%}{6.19}\right)}; R^2 = 0.9929 \quad (2)$$

$$C = 2.18 + \frac{6.10}{\left(1 + \frac{W_S\%}{8.27}\right)^{-0.55} + \left(1 + \frac{W\%}{8.27}\right)^{-5.75}}; R^2 = 0.9896 \quad (3)$$

Equations 1, 2 and 3 respectively reflect the mathematical relationship between water content and salinity and R_1 , R_2 , and C , and have a good fitting degree. (R_1 - $R^2=0.9976$, R_2 - $R^2=0.9929$, C - $R^2=0.9896$). Further inversion calculation of any two equations in equations 1, 2 and 3 can solve the calculation equation directly reflecting water content and salinity. In principle, any combination of R_1 , R_2 and C can reverse the calculation equation. However, due to the precision of the test equipment, it is

often difficult to accurately measure the capacitance C , and the action process of C itself is complicated [17, 23, 24]. In order to obtain a more accurate calculation equation, the equation with a better fitting degree is obtained in this paper. See equation 4 for details. Through simultaneous equations 1, 2 the calculation equations of salinity and water content are obtained:

$$\begin{cases} W_s\% = 30.06 \ln\left(\frac{R_2-8.55}{1662.93}\right) - 135.14 \ln\left(\frac{R_1+1697.36}{6773.11}\right) \\ W\% = 82.01 \ln\left(\frac{R_1+1697.36}{6773.11}\right) - 24.43 \ln\left(\frac{R_2-8.55}{1662.93}\right) \end{cases} \quad R^2 = 0.99 \quad (4)$$

3.5 Discussion on the equation of salinity, water content, and the equivalent circuit element

EIS method is used to carry out the inversion calculation on soil water content and salinity, and test calculation equations of soil water content and salinity are obtained. According to previous reports in [12,16,17,24], when the water content of the soil increases from 9% to 24%, R_1 of the soil decreases from 3868 to 1099 Ω , R_2 decreases from 331.42 to 23.26 k Ω , C of the soil increase from 0.94 to 29.90 μF . This study found a similar trend. In addition, R_1 and R_2 of soil have a significant logarithmic correlation with salinity (Tabs.3~5). In the past, the electrical impedance of soil was only a simple and rough response, and the comparability of test results was poor. At the same time, it does not constitute the actual soil electrical impedance value. On the contrary, EIS is used to express the water content and salinity of sulfate saline soil in this study. No pretreatment is needed to express the soil parameters. Although this study confirmed that sulfate saline soil is representative to some extent, it still needs to be further verified for other soil types.

ECM is the core part of EIS measurement, which is often closely linked to the microstructure changes of the measured object. In past research, the ECM of soils were analyzed and simplified, which is of profound significance to EIS measurement [17, 24]. In this study, the ECM (Fig.4) is designed to analyze and establish the significant relationship among water content, salinity, and circuit components, thus realizing the inversion calculation of salinity and water content of sulfate saline soil. The verification shows that the method is feasible [8].

The application of EIS will be more and more extensive. The EIS research conclusions presented in this paper are limited to the electrochemical response characteristics of sulfate saline soil prepared by ISO standard sand with 0-30% water content and 0-6% salinity. The changes in particle size, dry density, and salinity in sulfate saline soil also affect the electrical impedance of sulfate saline soil, which needs to be verified by further study.

4. CONCLUSION

Based on EIS, electrical impedance variations of sulfate saline soil with different water content and salinity are studied, and the corresponding ECM is analyzed, and the mathematical relationship between circuit elements and water content and salinity is obtained, and corresponding prediction equations of water content and salinity and prediction equations under the combined action are proposed. The specific conclusions are as follows:

(1) Electrical impedance characteristics of sulfate saline soil are studied by the EIS test, and the ECM of sulfate saline soil with the main component of sodium sulfate is analyzed. The proposed ECM provides a more reasonable analysis basis for EIS maps of sulfate saline soil, contributing to the comprehensive understanding of sulfate saline soil.

(2) The results show that R_1 and R_2 values of sulfate saline soil samples with the same thickness ($L = 10\text{cm}$) decrease with the increase of salinity and water content, while C increases with the increase of salinity and water content, and both values are exponentially related to salinity and water content. The effect of water content on test results is more prominent than that of salinity. The effect of salinity and water content on R_1 is more prominent than that of R_2 .

(3) EIS technology has no stress disturbance and it is a nondestructive, efficient and real-time method. To achieve more efficient characterization of detection, prediction equations for water content and salinity of sulfate saline soil are established. Inversion calculation of water content and salinity can be realized through measurement of R_1 and R_2 , and a method of establishing a corresponding prediction model is provided. Therefore, this study is of great significance for the research and treatment of soil salt expansion and the development of EIS technology.

ACKNOWLEDGMENT

This project is supported by the Natural Science Foundation of China (No. 51508579, 51674287).

References

1. Y.Z. Xu, *Building. Industry. Press.*, (1993). Beijing, China.
2. Z. Xiao, Y. Lai, Y.Z. Xu, M. Zhang, *Arab. J. Sci. Eng.*, 42 (2017) 3923
3. F. Klouche, K. Bendani, A. Benamar, H. Missoum, and N. Laredj, *Innovative. Infrastructure. Solutions.*, 3(2018) 1.
4. P. Rengasamy, *Funct. Plant. Biol.*, 37 (2010) 613.
5. P. Rengasamy, *J. Exp. Bot.*, 57 (2006) 1017.
6. C. Foncea, P. Acevedo, and R. Olguin, Geotechnical characterization of saline soils, *Proceedings of 16th ISMGE.*, Japan.9 (2005) 505.
7. L.L. Nan, and Q. Guo, *Acta. Ecologica. Sinica.*, (2018).
8. K.T.Osman, *Springer. International. Publishing.*,(2018) 255.
9. K. Wang, and M.J. Zhao, *Adv. Mater. Res.*, 726 (2013) 3877.
10. J.M. Cruz, I.C. Fita, L. Soriano, J. Paya, and M.V. Borrachero, *Cem. Concr. Res.*, 50 (2013) 51.
11. P. Han, P.J. Han, Y.B. Yan, and X.H. Bai, *Int. J. Electrochem. Sci.*, 13 (2018) 10548
12. P. Han, Y. Zhang, F.Y. Chen, and X. Bai, *J. Cent. South. Univ.*, 22 (2015) 4318.
13. S. Wansom, S. Janjaturaphan, S. Sinthupinyo, *Cem. Concr. Res.*, 40 (2010) 1714.
14. J.C. Hu, H.F. Wang, X.M. Sun, M.C. He. *Chinese J. Rock. Mech. Eng.*, 25 (2006) 1898.
15. S.M. Park, and J.S. Yoo, *Analytical. Chem.*, 75 (2003) 455A.
16. B. Evgenjj, J.R. Macdonald, *John Wiley and Sons, Inc.*, (2005). Canada
17. G.L. Song, *Cem. Conc. Res.*, 30 (2000) 1723.
18. H. Dong, L. Chen, and X.Z. Jiang, *J. Rock. Mech. Eng.*, A02 (2017) 4134.
19. B. He, P.J. Han, C.H. Lu, X.H. Bai, *Mater. Sci.*, 51 (2016) 890.
20. G. Pandey, R. Kumar, and R.J. Weber, Real Time Detection of Soil Moisture and Nitrates Using On-Board In-Situ Impedance Spectroscopy, *IEEE International Conference on Systems.* Manchester, England. (2013)1081.
21. D. Lesmes, *J. Appl. Electrochem.*, 39 (2003) 2129.
22. ASTM Committee D-18 on Soil and Rock, *ASTM International.*, 2011.

23. J.B. Jorcin, M.E. Orazem, P. Nadine, and B. Tribollet, *Electrochimica Acta.*, 51 (2006) 1473.
24. P. Gu, P. Xie, and J.J. Beaudoin, *Cem. Concr. Res.*, 23 (1993) 581.
25. D. Bao, and F. Kofi, *Geophysics*, 76 (2011) F329.
26. P. Gu, P. Xie, J.J. Beaudoin, *Cem. Concr. Res.*, 22 (1992) 833.
27. P. Gu, P. Xie, J.J. Beaudoin, *Cem. Concr. Res.*, 23 (1993) 157.
28. E.P. Nicolopoulou, F.E. Asimakopoulou, I.F. Gonos, and I.A. Stathopoulos, *Electr. Pow. Syst. Res.*, 113 (2014) 180.
29. L.M. Dudley, S. Bialkowski, and D. Or, *Soil. Sci. Soc. Am. J.*, 68 (2003) 518.
30. N.N. Deepakr, *Cement. Concrete. Comp.*, 44 (2013) 58.

© 2019 The Authors. Published by ESG (www.electrochemsci.org). This article is an open access article distributed under the terms and conditions of the Creative Commons Attribution license (<http://creativecommons.org/licenses/by/4.0/>).